JOURNAL OF MOLECULAR SPECTROSCOPY **189,** 1–7 (1998)
ARTICLE NO. MS977516

Hyperfine Structure of Rotation-Inversion Levels in the Excited ν_2 State of Ammonia

S. P. Belov,* Š. Urban,†,‡ and G. Winnewisser*

*I. Physikalisches Institut, Universität zu Köln, D-509 37 Köln, Germany; †J. Heyrovský Institute of Physical Chemistry, Academy of Sciences of the Czech Republic, Dolejškova 3, 182 23 Praha 8, Czech Republic; and ‡Institute of Chemical Technology, Technická 5, 166 28, Praha 6, Czech Republic

Received May 2, 1997; in revised form January 9, 1998

Hyperfine structures of the rotation–inversion transitions with $J = 3 \leftarrow 2$, $s \leftarrow a$, and $K = 0$, 1, 2, and with $J = 0 \leftarrow 1$, $a \leftarrow s$, and $K = 0$ in the excited ν_2 vibrational state have been resolved and measured by sub-Doppler saturation spectroscopy using the Cologne terahertz spectrometer with an accuracy of about 1 kHz. The line frequencies of the hyperfine structures of the rotation inversion transitions (at 466, 769, 742, and 763 GHz) have been simultaneously analyzed with the previously published $J = 2 \leftarrow 1$, $s \leftarrow a$, $K = 1$, ν_2 transition in terms of effective nuclear quadrupole and spin–rotation parameters. The corresponding pure rotation–inversion frequencies, deperturbed from the hyperfine effects, have also been derived.

1. INTRODUCTION

Ammonia ranges among the most studied species in molecular spectroscopy. Ammonia is an excellent example of a nonrigid molecule with a double minimum potential energy surface exhibiting a well known inversional splitting of energy levels. It played an important role for understanding the quantum mechanical tunneling effect (*1*). From the experimental point of view, ammonia has several primacies: it was the first molecule observed in microwave spectroscopy (*2, 3*), its transitions were used in the first maser (*4, 5*), and it was the first polyatomic molecule observed in the interstellar space (*6*). In addition, ammonia was used in introducing special spectroscopic techniques such as double resonance, laser Stark spectroscopy, and others.

The ground state hyperfine measurements of ammonia have significantly contributed to the development of the maser beam techniques (*7–8*), and the analysis of its spectrum has led to a full understanding of the quadrupole, spin–rotation, and spin–spin interactions in polyatomic molecules (*9–12*). The hyperfine structures have also been measured for the isolated transitions pertaining to the ν_2 (*13*), $2\nu_2$, and ν_4 (*14*) vibrational states. However, since only individual rotation–vibration or rotation transitions were measured, the experimental data was not sufficient to allow the determination of the basic parameters contained in the hyperfine Hamiltonian for the excited states.

In this study we present four rotation–inversion transitions in the excited ν_2 vibrational state that were measured using the Lamb dip method. This sub-Doppler saturation technique has allowed us to resolve the hyperfine structures of these submillimeter transitions for the first time. This data, together with data previously published, has been simultaneously analyzed to yield parameters of the effective hyperfine Hamiltonians for the two inversional components of the ν_2 vibrational state.

2. EXPERIMENTAL DETAILS AND RESULTS

The Lamb dip spectra (see Figs. 1 and 2) have been measured using the Cologne terahertz spectrometer that is described in some detail in Ref. (*15*). Tunable backward wave oscillators (BWO) OB-32 and OB-80 have been used to obtain saturation spectra. The detector used is a magnetically tuned QMC ''hot carrier'' InSb bolometer cooled by liquid He. The ammonia spectra have been recorded using a 3.9-m-long absorption cell with 10-cm inner diameter in a flow system with argon as a buffer gas to ensure low ammonia pressures of about 4 μbar and in turn minimize pressure shifts. More detailed description of this saturation experiment can be found in Refs. (*16, 17*).

A typical example of a well resolved sub-Doppler spectrum is presented in Fig. 1 where the linewidths (fwhm) of the hyperfine components of a rotation transition are about 100 kHz. This linewidth is greater then the expected homogeneous broadening.[1] We assume that the enhanced linewidths are caused by unresolved spin–spin interactions (see later or Refs. (*10–12*)). In addition to the hyperfine transitions, so-called cross-over resonance dips occur (*16–18*) for each pair of transitions that share one common level (upper

[1] In our case, the homogeneous broadening involves, above all, the saturation and pressure effects. For the rotational transition $J = 4 \leftarrow 3$ of the CO molecule, the linewidth measured with the same experimental setup was 25 kHz only.

0022-2852/98 $25.00

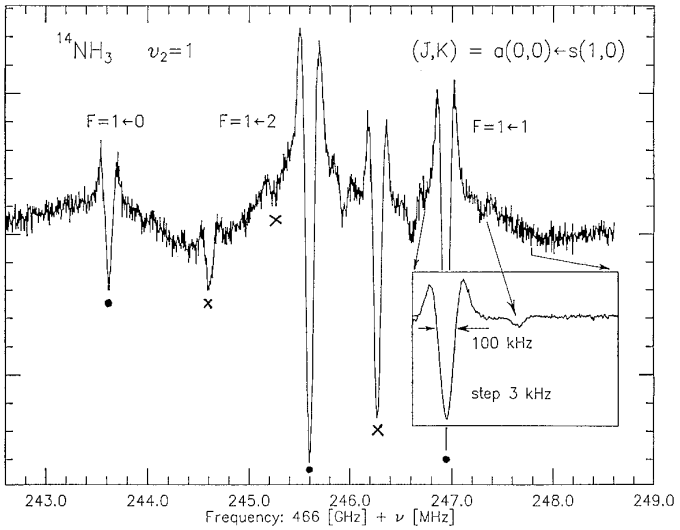

FIG. 1. Saturation dip spectrum of the $J = 1 \leftarrow 0$ rotational–inversional transition in the ν_2 excited vibrational state of $^{14}NH_3$ around 466.246 GHz. The three hyperfine components are marked by ●; the cross-over resonances (see Fig. 3) are marked by crosses. The line width of all lines (fwhm) is about 100 kHz.

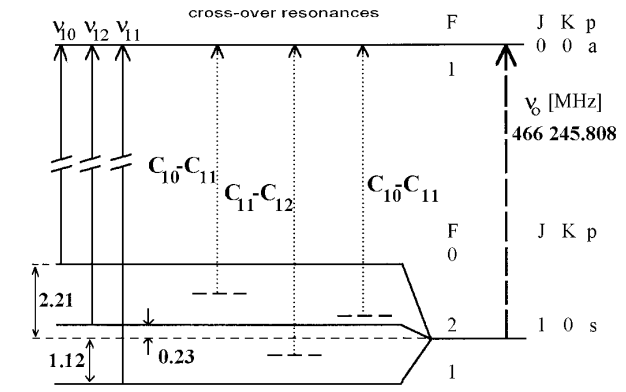

FIG. 3. Energy diagram of the two lowest rotational–inversional levels in the ν_2 excited vibrational state of $^{14}NH_3$. Half of the inversional doublets are missing due to zero values of nuclear spin statistic weights. The cross-over resonances are identified using the notation $C_{F'F''}$–$C_{F'F''}$ indicating the upper and lower $F1$ values of both transitions $\nu_{F'F''}$.

or lower) and that overlap within their Doppler widths. These are marked in the spectra on Figs. 1 and 2 by crosses. The positions of these cross-over peaks (*16–18*) occur exactly between two hyperfine components having the same common level (see Figs. 3 and 4), and their frequencies can therefore be used to check the experimental accuracy. From this comparison, the experimental accuracy is estimated to be about 1 kHz for well developed isolated lines. This value corresponds to our previous studies (e.g., *16* and *17*). The accuracy of bad or overlapped lines was estimated individually (see the second column of Table 1). It should be noted

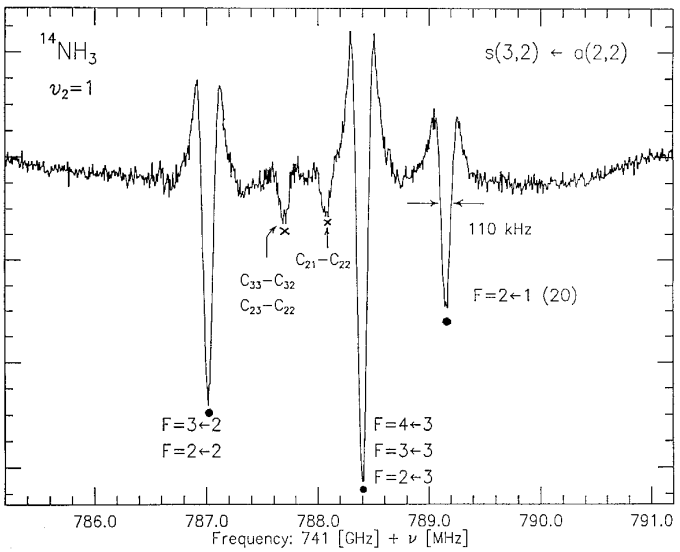

FIG. 2. Saturation dip spectrum of the $J = 3 \leftarrow 2$, $K = 2$, $s \leftarrow a$ rotational-inversional transition in the ν_2 excited vibrational state of $^{14}NH_3$ around 741.788 GHz. The three resolved hyperfine lines are marked by ●; the cross-over resonance dips (see Fig. 4) are marked by crosses, and they are identified using the notation $C_{F'F''}$–$C_{F'F''}$ indicating the upper and lower $F1$ values of both transitions.

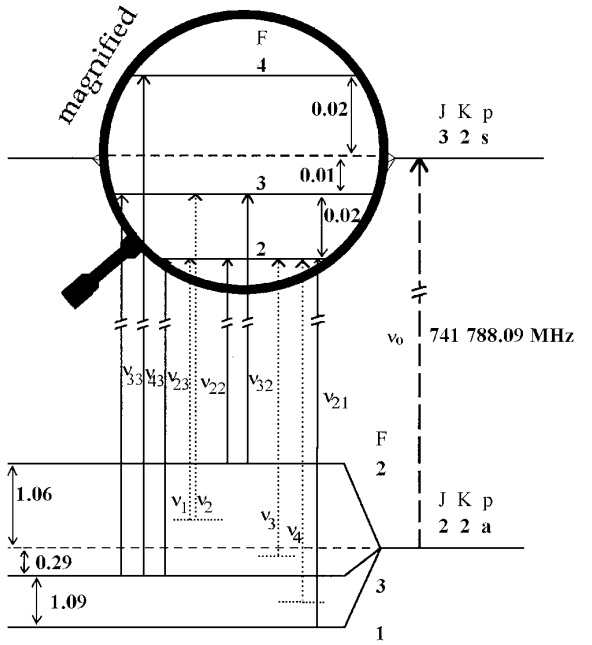

FIG. 4. Energy diagram of levels that are involved in the $J = 3 \leftarrow 2$, $K = 2$, $s \leftarrow a$ rotational-inversional transition in the ν_2 excited vibrational state of $^{14}NH_3$. The averaged molecular field gradient q_J vanishes for the $(J, K) = (3, 2)$, and therefore the quadrupole splitting of the upper state vanishes. The analyzed spacing between the levels with the different$_{F1}$ values corresponds to the N-spin–rotation interaction effect. The cross-over resonances are marked by ν_1, ν_2, ν_3, and ν_4, which correspond to the labels C_{23}–C_{22}, C_{33}–C_{32}, C_{22}–C_{21}, and C_{23}–C_{21}, respectively, in the notation indicating the upper and lower $F1$ values of both transitions $\nu_{F'F''}$.

TABLE 1

Experimental and Calculated Hyperfine Frequencies of Ammonia in the ν_2 Vibrational State

$p' J' K' F' \leftarrow p'' J'' K'' F''$	ν_{exp} [MHz][a]	ν_{corr} [MHz][a]	ν_{calc} [MHz]	$\Delta\nu$[MHz]	Inten. [r.u.]	$\Delta E'_{hf}$	$\Delta E''_{hf}$
$a\,0\,0\,1 \leftarrow s\,1\,0\,0$	466243.620(001)	466243.620(002)	466243.620	0.000	4.00	0.000	2.210
$a\,0\,0\,1 \leftarrow s\,1\,0\,2$	466245.597(001)	466245.605(005)	466245.603	0.002	20.00	0.000	0.227
$a\,0\,0\,1 \leftarrow s\,1\,0\,1$	466246.940(001)	466246.945(003)	466246.946	-0.001	12.00	0.000	-1.116
$s\,3\,2\,2 \leftarrow a\,2\,2\,1$	741789.156(001)	741789.155(002)	741789.155	0.000	252.00	-0.022	-1.089
$s\,3\,2\,4 \leftarrow a\,2\,2\,3$	741788.400(005)	741788.397(006)	741788.396	0.001	540.00	0.016	-0.292
$s\,3\,2\,3 \leftarrow a\,2\,2\,3$	741788.400(050)	741788.399(050)	741788.375	0.024	46.67	-0.005	-0.292
$s\,3\,2\,2 \leftarrow a\,2\,2\,3$	741788.400(100)	741788.403(100)	741788.358	0.045	1.33	-0.022	-0.292
$s\,3\,2\,4 \leftarrow a\,2\,2\,3$	741788.401(005)[d]	741788.398(005)	741788.396	0.002	540.00	0.016	-0.292
$s\,3\,2\,3 \leftarrow a\,2\,2\,3$	741788.389(050)[d]	741788.388(050)	741788.375	0.013	46.67	-0.005	-0.292
$s\,3\,2\,2 \leftarrow a\,2\,2\,3$	741788.352(100)[d]	741788.355(050)	741788.358	-0.003	1.33	-0.022	-0.292
$s\,3\,2\,3 \leftarrow a\,2\,2\,2$	741787.017(005)	741787.015(005)	741787.020	-0.005	373.33	-0.005	1.062
$s\,3\,2\,2 \leftarrow a\,2\,2\,2$	741787.017(050)	741787.020(050)	741787.004	0.016	46.67	-0.022	1.062
$s\,3\,2\,3 \leftarrow a\,2\,2\,2$	741787.021(005)[d]	741787.019(010)	741787.020	-0.001	373.33	-0.005	1.062
$s\,3\,2\,2 \leftarrow a\,2\,2\,2$	741786.984(050)[d]	741786.987(050)	741787.004	-0.017	46.67	-0.022	1.062
$s\,3\,1\,3 \leftarrow a\,2\,1\,3$	762851.494(020)	762851.494(020)	762851.497	-0.003	46.67	-0.836	0.166
$s\,3\,1\,4 \leftarrow a\,2\,1\,3$	762852.622(020)	762852.624(025)[c]	762852.626	-0.002	252.00	0.642	0.516
$s\,3\,1\,2 \leftarrow a\,2\,1\,1$	762852.622(020)	762852.624(030)[c]	762852.626	-0.002	540.00	0.293	0.166
$s\,3\,1\,2 \leftarrow a\,2\,1\,3$	762852.940(050)	762852.942(050)[c]	762852.975	-0.033	1.33	0.642	0.166
$s\,3\,1\,3 \leftarrow a\,2\,1\,2$	762852.204(001)	762852.209(005)	762852.206	0.003	373.33	-0.836	-0.542
$s\,3\,1\,2 \leftarrow a\,2\,1\,2$	762853.670(005)	762853.684(005)	762853.684	0.000	46.67	0.642	-0.542
$s\,3\,0\,4 \leftarrow a\,2\,0\,3$	769710.300(010)	769710.287(015)[c]	769710.287	0.000	540.00	0.360	0.319
$s\,3\,0\,3 \leftarrow a\,2\,0\,2$	769710.300(030)	769710.281(035)[c]	769710.286	-0.005	373.33	-1.038	-1.078
$s\,3\,0\,4 \leftarrow a\,2\,0\,3$	769710.302(010)[e]	769710.289(015)	769710.287	0.002	540.00	0.360	0.319
$s\,3\,0\,3 \leftarrow a\,2\,0\,2$	769710.296(020)[e]	769710.277(025)	769710.286	-0.009	373.33	-1.038	-1.078
$s\,3\,0\,2 \leftarrow a\,2\,0\,1$	769710.012(005)	769710.000(010)	769709.999	0.001	252.00	0.804	1.052
$s\,3\,0\,3 \leftarrow a\,2\,0\,3$	769708.887(010)	769708.896(020)	769708.889	0.007	46.67	-1.038	0.319
$s\,3\,0\,2 \leftarrow a\,2\,0\,3$	769710.630(500)	769710.630(500)[c]	769710.731	-0.101	1.33	0.804	0.319
$s\,3\,0\,2 \leftarrow a\,2\,0\,2$	769712.140(010)	769712.123(015)	769712.129	-0.006	46.67	0.804	-1.078
$s\,2\,1\,2 \leftarrow a\,1\,1\,1$	140140.795(060)[b]	140140.794(060)	140140.786	0.008	90.00	-0.582	0.516
$s\,2\,1\,1 \leftarrow a\,1\,1\,1$	140141.900(250)[b]	140141.902(250)[c]	140141.928	-0.026	30.00	0.561	0.516
$s\,2\,1\,1 \leftarrow a\,1\,1\,2$	140142.152(500)[b]	140142.163(500)[c]	140142.542	-0.379	2.00	0.561	-0.098
$s\,2\,1\,3 \leftarrow a\,1\,1\,2$	140142.152(025)[b]	140142.150(025)	140142.157	-0.007	168.00	0.176	-0.098
$s\,2\,1\,2 \leftarrow a\,1\,1\,2$	140141.420(060)[b]	140141.427(060)	140141.399	0.028	30.00	-0.582	-0.098
$s\,2\,1\,1 \leftarrow a\,1\,1\,0$	140143.495(030)[b]	140143.503(030)	140143.502	0.001	40.00	0.561	-1.058

[a] Uncertainties in parentheses are in the units of the last reported digits.

[b] Experimental frequencies from Ref. (*13*). The uncertainties are relative. The absolute uncertainties are about 60 kHz.

[c] Strongly overlapped lines.

[d] Semi-experimental frequencies (see text) obtained using the following cross-over peak frequencies (see Figs. 2 and 4): $\nu[C_{22}-C_{21}] = 741\,788.070(10)$ MHz, $\nu[C_{22}-C_{23}] = \nu[C_{32}-C_{33}] = 741\,787.698(50)$.

[e] Semi-experimental frequencies (see text) obtained using the following cross-over peak frequencies: $\nu[C_{32}-C_{33}] = 769\,711.218(10)$, $\nu[C_{33}-C_{32}] = \nu[C_{33}-C_{43}] = 769\,709.595(20)$.

that the accuracy of the peak maxima is not directly used for the determination of statistical weights in a least square fit. For this purpose, proton internal splittings of individual lines have been approximately evaluated (see further).

In some cases, the cross-over peaks can provide valuable information on the hyperfine structures (e.g., *18*). For example, the hyperfine structure of the $s(3, 2) \leftarrow a(2, 2)$ rotation–inversion transition is not fully resolved (Figs. 2 and 4) because of a negligible nuclear quadrupole splitting in the $J = 3$, $K = 2$ rotational level (the averaged value of the molecular field gradient vanishes for these rotational quantum numbers, see Eq. [3]), and the cross-over peaks can effectively increase the spectral resolution in this case. Since the frequency of the cross-over peaks should be exactly between the frequencies of the transitions having the same upper or lower level, we can calculate, for instance, the transition frequency of the $F = 2 \leftarrow 2$ component (which is overlapped) from the frequencies of the well resolved $F = 2 \leftarrow 1$ component and the corresponding cross-over peak (see Figs. 2 and 4, the corresponding cross-over peak is marked by $C_{21}-C_{22}$). Using the calculated intensities of the individual hyperfine components (*19*), the frequencies of the remaining overlapped hyperfine components can be step by step estimated (see also Fig. 4). These ''semi-experimental'' frequencies derived for

the overlapped components using the cross-over peaks were also used in this study. However, the uncertainties of these semi-experimental frequencies are larger, partly because of the low intensities of some cross-over lines, partly due to the complex structures of the overlapping lines.

In the present study, we have measured hyperfine structures of four rotation–inversion transitions in the excited ν_2 vibrational state. All the pure experimental as well as semi-experimental frequencies of all the hyperfine components are given in the second column of Table 1. The frequencies of the selected cross-over peaks used in this study are given in a footnote to this table.

3. THEORY AND ANALYSIS OF DATA

Because of the small number of rotation–inversion transitions measured in the excited vibrational state under sub-Doppler resolution, we did not perform a detailed analysis of rotation inversion levels in this paper. To warrant such a study, an extensive set of new precise data is required, which must be measured using the most advanced experimental techniques. Therefore, the present study focuses only on the analysis of the hyperfine structures of the ν_2 vibrational state.

The effective hyperfine structure Hamiltonian for the ν_2 vibrational state of ammonia can be written analogously to that of the ground state (*11, 12*):

$$\begin{aligned}\mathbf{H}_{\text{eff}} &= Q^*[2I_N(2I_N-1)(2J-1)2J]^{-1}\\ &\times\{3(I_N\cdot J)^2+1.5(I_N\cdot J)-I_N^2J^2\}+R(I_N\cdot J)\\ &+S(I_H\cdot J)+T\,3[2J-1)(2J+3)]^{-1}(I_N\cdot J)\\ &\times(I_H\cdot J)+U\,2[(2J-1)(2J+3)]^{-1}\\ &\times\{3(I_H\cdot J)^2+1.5(I_H\cdot J)-I_H^2J^2\},\end{aligned}\qquad[1]$$

where the coupling parameters Q^*, R, S, T, U, and the corresponding operators are related to the nitrogen quadrupole, nitrogen spin–rotation, hydrogen spin–rotation, nitrogen–hydrogen spin–spin, and mutual hydrogen spin–spin interactions, respectively. The operators provide both the diagonal and off-diagonal matrix elements on the basis of the symmetric top rotational wave functions (*11, 19*). The effect of the off-diagonal matrix elements of the hyperfine operators with respect to our set of experimental hyperfine frequencies with low values of rotational quantum number J (see Table 1) is, however, negligible; the corresponding parameters were not determinable and therefore they will not be considered in the following text.

The hydrogen spin–rotation and all spin–spin magnetic interactions in the ν_2 vibrational state are obviously similar to those that were found in the ground state (*10, 11*) since no corresponding splittings have been resolved in our spectra. Therefore, these operator terms were neglected in our effective Hamiltonian, however, their effect was respected in the estimation of the statistical weights and for fine corrections of the experimental frequencies. On the other hand, to obtain a full quantitative description of all experimental data, the first order description of the nitrogen quadrupole operator has been extended by adding higher order effective quadrupole centrifugal distortion terms to absorb the rotation vibration interactions, above all the huge Coriolis interactions between the ν_2 and ν_4 vibrational states (*20*). It means, for the analysis of the observed spectra, the following effective Hamiltonian has been used:

$$\begin{aligned}\mathbf{H}_{\text{eff}} &= Q^*[2I_N(2I_N-1)2J(2J-1)]^{-1}\\ &\times\{3(I_N\cdot J)^2+1.5(I_N\cdot J)-I_N^2J^2\}\\ &\times\{1+\eta_JJ^2+\eta_KJ_z^2\}+R(I_N\cdot J),\end{aligned}\qquad[2]$$

where η_J and η_K are the effective quadrupole centrifugal parameters. The nitrogen quadrupole coupling parameter (Q^*) is usually expressed in terms of a product of the nuclear quadrupole moment (eQ) and the quantity q_J, which is an averaged value of the molecular field gradient in the direction of the Z-axis of the space fixed coordinate system (*11*). q_J is a function of the direction cosines, and in the case of a symmetric top molecule, this quantity can be expressed as a simple expression in the rotational quantum numbers:

$$q_J = q\{3K^2/[J(J+1)]-1\}J(2J+3)^{-1},\qquad[3]$$

where q is the molecular field gradient. The nitrogen spin-rotation coupling term R represents the magnetic interactions between the nitrogen spin magnetic and orbital momenta. Because of the ammonia axial molecular symmetry, two of the three interaction coefficients are equal ($C_x = C_y$), and thus the spin-rotation coupling term can be expressed in the following form:

$$R = [C_xJ^2+(C_z-C_x)J_z^2]J^{-2},\qquad[4]$$

where C_z is the remaining z component of the magnetic spin-orbital coupling. Therefore, the effective hyperfine operator used in the present analysis has the following form:

$$\begin{aligned}\mathbf{H}_{\text{eff}} &= eQq\{3K^2/[J(J+1)]-1\}\\ &\times[2I_N(2I_N-1)(2J-1)(2J+3)]^{-1}\\ &\times\{3(I_N\cdot J)^2+1.5(I_N\cdot J)-I_N^2J^2\}\\ &\times\{1+\eta_JJ^2+\eta_KJ_z^2\}\\ &+[C_x+(C_z-C_x)J_z^2J^{-2}](I_N\cdot J),\end{aligned}\qquad[5]$$

where $eQq\eta_J$ and $eQq\eta_K$ are parameters of the quadrupole centrifugal distortion terms. The matrix elements used in this study are listed in Refs. (*11, 12*) and (*19*).

The form of the effective Hamiltonian (Eq. [5]) corresponds to a basis set consisting of $(2I_N + 1)$ wave functions $|J, K, M_J, F, M_F\rangle$, where the corresponding operator F represents the vector sum of J and I_N, M_F is a quantum number related to the projection of F along the laboratory fixed Z direction, and I_N is the nitrogen spin quantum number (for ^{14}N, $I_N = 1$). This basis set was used to assign all the observed hyperfine components. The assignments have been checked using the calculated relative intensities.

The hydrogen–nitrogen spin–spin, as well as the hydrogen spin-orbital, interactions require an extension of the basis set $|J, K, M_J, F, M_F\rangle$ to respect the hydrogen spin multiplicity $2I_H + 1$ (where I_H is a hydrogen spin quantum number, $I_H = I_1 + I_2 + I_3 = \frac{1}{2}$ or $I_H = \frac{3}{2}$ for rotational states with $k = 3n \pm 1$ or $k = 3n$, respectively). In the standard approach, the total angular momentum operator $F' = F + I_H$ is introduced, which forms the extended basis $|J, K, M_J, F, M_F, F', M_F'\rangle$ (see Refs. (*9, 10*)). This basis set has been used for predictions of the unresolved proton spin structures to simulate their effect on peak maxima positions. In these calculations, we have used the theoretical *ab initio* values of the magnetic coupling parameters for the excited vibrational ν_2 state of ammonia from Ref. (*21*) and the corresponding matrix elements of the hydrogen spin coupling operators (see Eq. [1]) from Ref. (*10*). An envelope of the unresolved hyperfine components was then simulated by a numerical superposition of all possible fine transitions and cross-over peaks. In the simulation procedure, simple Lorenz profiles, calculated relative intensities (*10*), and linewidths (fwhm) of 80 kHz were used. The 80-kHz linewidth has been selected because it forms the observed linewidth about 100 kHz for the $F = 1 \leftarrow 1$ component of the $J = 0 \leftarrow 1$ rotational transition (see Fig. 1). These calculations have shown weak shifts of the line maxima in a frequency ranging from 0 to ± 20 kHz that were used as a correction factor to the experimental frequencies (see Table 1) to minimize the influence of the neglected proton hf structures on the least square fit. The estimated shifts have been believed with 25% uncertainty, and, in addition to this, a 15-kHz error has been considered for the linewidths used in the simulation procedure. These data, together with the experimental accuracy, have been used to set appropriate statistical weights to all the hyperfine components (see the third column of Table 1).

RESULTS AND DISCUSSION

The measured frequencies of the hyperfine components of the four rotational inversional transitions and the experimental data measured by Hüttner and Majer (*13*) have been fitted to the effective Hamiltonian described above (Eq. [5]). The results of the fit are given in Table 1 from which it is obvious that all the frequencies are reproduced within the experimental uncertainties of the measured ones. The calculated hyperfine energy contributions to the upper and lower rotation–inversion levels, which completely describe the hyperfine splittings, are listed in the last two columns of Table 1. Two sets of the corresponding effective parameters were obtained for the $a\nu_2$ and $s\nu_2$ vibrational states and they are listed in Table 2.

TABLE 2
Effective Hyperfine Coupling Parameters of Ammonia in the Excited ν_2 Vibrational State[a]

Parameter	$s\nu_2$	$a\nu_2$
eQq	- 4.503 9 (33)	- 4.128 (67)
$eqQ\eta_J$	0.031 7 (11)	- 0.026 5(89)
$eqQ\eta_K$	- 0.266 (16)	- 0.023 9 (92)
C_N	0.005 41 (40)	0.006 65 (61)

[a] Parameters are given in MHz. Uncertainties in parentheses are in the units of the last reported digits

The nuclear quadrupole coupling constants eQq in the ν_2 vibrational state obtained in this study show a significant difference between the *a*- and *s*-inversional states. This difference is about 30 times larger with respect to the value in the vibrational ground state and can be compared with a SCF electric field gradient calculation performed by Fowler and Špirko (*22*). Their predicted values of eQq are -4.4540 and -4.2915 MHz for the *s*- and *a*-inversional ν_2 states, respectively. Our results agree quite well also with the previous experimental values of the corresponding matrix elements for the $|s, J = 1, K = 1\rangle$ and $|a, J = 1, K = 1\rangle$ rotation inversion states [$-4.438(18)$ and $-4.263(18)$ MHz] that have been determined for the ν_2 vibrational state by Hüttner and Majer (*13*).

From the two independent coupling coefficients, $C_N = C_x = C_y$ and $C_K = C_z$, of the spin orbital Hamiltonian, only one, C_N, has been determined (see Table 2) in this study. Our data set does not provide sufficient information to determine the linear combination of the coefficients $(C_K - C_N)$, see Eq. [5], which is probably too small and of negligible effect (below 5 kHz) with respect to our measurement accuracy of the hyperfine transitions. The situation in the ν_2 vibrational state can be analogous to the vibrational ground state where the values of the coefficients C_K^0 and C_N^0 have been experimentally determined [averaged values, $(a + s)/2$] at 6.708 and 6.807 kHz (*10*), respectively, with a difference of about -0.1 kHz. This assumption corresponds to the *ab initio* theoretical study (*21*) where the calculated $(C_K - C_N)$ differences are $+0.11$ and $+0.45$ kHz, for the ground and ν_2 vibrational states, respectively. The predicted small size of $C_K^{\nu_2} - C_N^{\nu_2}$ is consistent with the fact that it cannot be determined from our data set. On the other hand, the comparison of the calculated *ab initio* theoretical coeffi-

TABLE 3
Rotation-Inversion Frequencies of NH_3 in the ν_2 Vibrational State (deperturbed from the hyperfine interaction effects)

Transition	ν_{unp} [MHz][a]	$\nu_{p=0}$ [MHz][b]	$\tilde{\nu}_{p=0}$ [cm^{-1}][b]	$\tilde{\nu}_{calc}$ [cm^{-1}][c]
$a\,0\,0 \leftarrow s\,1\,0$	466 245.8303 (9)	466 245.8133 (16)	15.552 286 285 (53)	15.552 27 (2)
$s\,2\,1 \leftarrow a\,1\,1$	140 141.8834(84)[d,e]	140 141.8067 (230)[d]	4.674 627 50 (77)[d]	4.674 64 (2)
$s\,3\,2 \leftarrow a\,2\,2$	741 788.0878 (16)	741 788.0884 (17)	24.743 387 254 (57)	24.743 39 (2)
$s\,3\,1 \leftarrow a\,2\,1$	762 852 4992 (19)	762 852.4893 (20)	25.446 020 036 (66)	25.446 03 (2)
$s\,3\,0 \leftarrow a\,2\,0$	769 710.2459 (27)	769 710.2347 (28)	25.674 769 800 (93)	25.674 77 (2)

[a] Pure rotation–inversion frequencies derived from the hyperfine interaction data (Table 1) measured at the sample pressure ~4 μbar.

[b] Pure rotation vibration frequencies or wavenumbers corrected to the zero-pressure using data from Refs. (*23, 24*).

[c] Calculated wavenumbers using the energy levels taken from Ref. (*25*).

[d] Calculated from the hyperfine measurements in Ref. (*13*). In this study, the error of the absolute frequency is estimated to be 60 kHz and the sample pressure reported is about 26 μbar. The error of the pressure determination is assumed to be about 20%.

[e] The marked uncertainty is derived from the relative accuracy of the individual hyperfine components.

cients $sC_N^{\nu_2}$ and $aC_N^{\nu_2}$ (6.23 and 6.28 kHz in Ref. (*21*)) with the values in Table 2 determined in this study shows a good agreement.

It is obvious from Table 2 that all the *s* parameters are determined significantly better than the *a* parameters. This is because the most precise measured hyperfine structure of the $a(0, 0) \leftarrow s(1, 0)$ rotation inversion transition (see Fig. 1) determines the *s* parameters only. Higher uncertainty of the *a*-centrifugal parameters is then a natural consequence of the small extent of the experimental data analyzed (two different *J* values only).

In addition to the quadrupole and spin–orbital parameters presented in Table 2, the analysis of the hyperfine structures also leads to pure rotation–inversion frequencies, deperturbed from the effects of the quadrupole and magnetic (spin–orbit or spin–spin) interactions. The pure rotation–inversion frequencies obtained in this study are listed in Table 3. These deperturbed frequencies represent the most precise input data for determination of the rotational Hamiltonian parameters. It should be noted that in the case of nonresolved hyperfine structures, the frequency of the peak maximum (the center of gravity of the absorption that results from a superposition of the individual hyperfine components) does not correspond, in general, to the frequency of the pure (deperturbed) rotation–inversion transition.

While the accuracy of our measurements is estimated to be about 1 kHz, the same accuracy cannot be set for the rotation–inversion frequencies because of the effects of the pressure shifts of lines. The experimental uncertainties marked for the frequencies in the second column of Table 3 express an accuracy of the frequency determination from the hyperfine data at the experimental sample pressure (~4 μbar)[2]. The pressure shifts of low-*J* rotation-inversion transitions in the ν_2 vibrational state are anomalously large, about 0.1–5 GHz/bar (*23*), and this fact increases the absolute uncertainties of the ''zero-pressure'' rotation inversion frequencies. It is obvious that knowledge of the pressure shifts can improve these uncertainties.

The pressure shifts of the rotation inversion transitions investigated in this study have been experimentally determined (*23, 24*), and the pressure dependencies obtained were described using the following linear equation:

$$\nu = \nu_0 + bp, \qquad [6]$$

where *p* is the sample pressure and *b* are experimental parameters that are different for the individual rotation inversion transitions. The measured values of the *b* parameters are 4.24, 2.94, 2.80, 2.47, and −0.15 GHz/bar for the rotation inversion transitions $a(0,0) \leftarrow s(1,0)$, $s(2,1) \leftarrow a(1,1)$, $s(3,0) \leftarrow a(2,0)$, $s(3,1) \leftarrow a(2,1)$, and $s(3,2) \leftarrow a(2,2)$, respectively (*23, 24*). These parameters make it possible to calculate the correction factors [−0.0170, −0.0767[2], −0.0118, −0.0099, and 0.0006 MHz] to obtain the zero-pressure frequencies (or wavenumbers; see the third and fourth column of Table 3). The 5% uncertainties of the pressure correction factors were assumed (see also footnote 2).

The last column of Table 3 presents the wavenumbers calculated from the molecular parameters obtained from an

[2] The experimental sample pressure for the transition $J = 2 \leftarrow 1$, $s \leftarrow a$, $K = 1$ measured by Hüttner and Majer in Ref. (*13*) was about 2.6 Pa (26 μbar). Since the pressure information in Ref. (*13*) is not explicitly fixed to the measured frequency, a 20% uncertainty is assumed.

extensive analysis of experimental data measured more than 12 years ago (*25*). Their agreement with the zero-pressure wavenumbers obtained in this study is very good and corresponds to the uncertainties quoted in Ref. (*25*). However, on the other hand, the new data improve the accuracy by about two orders of magnitude.

Strictly speaking, the pressure dependence of the hyperfine splittings could be also considered as a consequence of the nonzero matrix elements that are off-diagonal in the symmetric-top wavefunction basis. However, with respect to the negligible contributions of these off-diagonal matrix elements to the hyperfine energies of our low-J data, we believe that these pressure effects on the hyperfine structure are negligible and below the limit of our data accuracy.

ACKNOWLEDGMENTS

The work in Cologne was supported in part by DFG through a special grant, SFB-301. Š.U. gratefully acknowledges financial support from the EC (Contract No. CHRXCT 930157 and its supplementary agreement ERB-CIPDCT 940614) and from grant No. 303/96/0946 of the Grant Agency of the Czech Republic. We also thank Dipl. Phys. Thomas Klaus for assistance during the course of this work and Dr. Vladimír Špirko for helpful criticism of the manuscript.

REFERENCES

1. D. M. Dennison and G. E. Uhlenbeck, *Phys. Rev.* **41,** 313–321 (1932).
2. C. E. Cleeton and N. H. Williams, *Phys. Rev.* **45,** 234–237 (1934).
3. B. Bleaney, *in* ''Amazing Light,'' (Y. Chiao, Ed.), pp. 79–86, Springer, New York, 1996.
4. J. P. Gordon, H. J. Zeiger, and C. H. Townes, *Phys. Rev.* **95,** 282–284L (1954).
5. J. P. Gordon, H. J. Zeiger, and C. H. Townes, *Phys. Rev.* **99,** 59–66 (1955).
6. A. C. Cheung, D. M. Rank, C. H. Townes, D. D. Thornton, and J. Welch, *Phys. Rev. Letters* **21,** 1701–1705 (1968).
7. G. R. Gunther-Mohr, R. L. White, A. L. Schawlow, W. E. Good, and D. K. Coles, *Phys. Rev.* **94,** 1184–1190 (1954).
8. J. P. Gordon, *Phys. Rev.* **99,** 1253–1263 (1955).
9. G. F. Hadley, *Phys. Rev.* **108,** 291–293 (1957).
10. S. G. Kukolich, *Phys. Rev.* **156,** 83–92 (1967).
11. G. R. Gunther-Mohr, C. H. Townes, and J. H. Van Vleck, *Phys. Rev.* **94,** 1191–1203 (1954).
12. J. T. Hougen, *J. Chem. Phys.* **57,** 4207–4217 (1972).
13. W. Hüttner and W. Majer, *Mol. Phys.* **52,** 631–636 (1984).
14. W. H. Weber and R. W. Therune, *J. Chem. Phys.* **78,** 6422–6436 (1983).
15. G. Winnewisser, *Vibrational Spectrosc.* **8,** 241–253 (1995).
16. G. Winnewisser, S. P. Belov, Th. Klaus, and Š. Urban, *Z. Naturforsch.* **51a,** 200–206 (1996).
17. S. P. Belov, Th. Klaus, G. M. Plummer, R. Schieder, and G. Winnewisser, *Z. Naturforsch.* **50a,** 1187–1190 (1995).
18. G. Magerl, W. Schupita, J. M. Frye, W. A. Kreiner, and T. Oka, *J. Mol. Spectrosc.* **107,** 72–83 (1984).
19. H. P. Benz, A. Bauder, and Hs. H. Günthard, *J. Mol. Spectrosc.* **21,** 156–164 (1966).
20. Š. Urban, V. Špirko, D. Papoušek, R. S. McDowell, N. G. Nereson, S. P. Belov, L. I. Gerhstein, A. V. Maslovskij, A. F. Krupnov, J. Curtis, and K. N. Rao, *J. Mol. Spectrosc.* **79,** 455–495 (1980).
21. J. Oddershede, I. Paidarová, and V. Špirko, *J. Mol. Spectrosc.* **152,** 342–354 (1992).
22. P. Fowler and V. Špirko, *J. Chem. Soc. Faraday Trans.* **86,** 1991–1994 (1990).
23. S. P. Belov, L. I. Gershtein, A. F. Krupnov, A. V. Maslovskij, Š. Urban, V. Špirko, and D. Papoušek, *J. Mol. Spectrosc.* **84,** 288–304 (1980).
24. S. P. Belov, A. F. Krupnov, and A. A. Mel'nikov, *Izv. VUZov, Radiofiz. (in russian)* **25,** 718–720 (1981).
25. Š. Urban, Romola D'Cunha, K. N. Rao, and D. Papoušek, *Canad. J. Phys.* **62,** 1775–1791 (1984).